



Naphthyridine–imidazole hybrid ligands for the construction of multinuclear architecture

S.M. Wahidur Rahaman, Dipak Das, Nabanita Sadhukhan, Arup Sinha, Jitendra K. Bera *

Department of Chemistry, Indian Institute of Technology Kanpur, Kanpur 208016, India

ARTICLE INFO

Article history:

Available online 13 March 2011

Dedicated to Professor Wolfgang Kaim

Keywords:

Self-assembly
Metallamacrocycle
Naphthyridine
Rhodium
Coordination polymer

ABSTRACT

Reaction of 2-imidazolyl-5,7-dimethyl-1,8-naphthyridine (L^1) with $[\text{Rh}(\text{COD})\text{Cl}]_2$ (COD = 1,5-cyclooctadiene) affords the dinuclear complex $[\text{Rh}(\text{COD})\text{Cl}]_2(\mu-L^1)$ (**1**). Elimination of chloride from the metal coordination sphere leads to a self-assembled tetranuclear macrocycle $[\text{Rh}(\text{COD})L^1]_4[\text{ClO}_4]_4$ (**2**). A subtle alteration in the ligand framework results in the polymeric chain compound $\{\text{Rh}(\text{COD})(L^2)\}_n(\text{PF}_6)_n$ (**3**) (L^2 = 2-imidazolyl-3-phenyl-1,8-naphthyridine). In all these complexes, the imidazole nitrogen and one of the naphthyridine nitrogen (away from the imidazole substituent) bind the metal. The 'parallel' and 'perpendicular' dispositions of nitrogens are observed in these compounds contributing to different Rh...Rh separations. The L^1 ligand adopts planar configuration, whereas the naphthyridine–imidazole rings deviate from planarity in L^2 yielding a polymeric structure. The extent of deviation is less in the polymeric structure $\{\text{Mo}_2(\text{OAc})_4(L^2)\}_n$ (**4**) in which the ligand exhibits weak axial interactions to the metal.

© 2011 Elsevier B.V. All rights reserved.

1. Introduction

The desire to make new and complex structures has been a motivating factor for the intensive study of metal-supramolecular chemistry. The applications of metal-containing supramolecular assemblies in gas storage [1–4], catalysis [5–8], single-molecule-magnetism [9–11], separation [12–14], sensor [15–18] and many other areas have afforded credence to this chemistry. Numerous multitopic ligands have been designed and metal components (including secondary building units, or SBU) have been developed [19–21]. Pyridine based ligands were one of the first to be used in the construction of metallamacrocycles [22–24]. Multi-site ligands containing multiple imidazole units have also been used in recent years [25,26]. The general scheme employed for the ligand design involves the covalent attachment of donor units on a desired organic platform. Ligand systems incorporating different types of donor moieties have shown prospects for the construction of homo- and heterometallic metallamacrocycles. Pyridine carboxylic acid has been employed for the construction of Pt and Pd based molecular squares [27,28]. Dunbar et al. have reported several heterobimetallic metallacycles consisting of Re_2/Pt and Re_2/Zn units [29,30]. Imidazole carboxylic acids have been employed for the construction of molecular polygons with 'Cp'Rh' corners [31]. The disposition of metal-binding sites in the ligand framework and the directionality of the metal precursor dictate the topology

of the resultant structure. The present work describes our recent effort to synthesize multinuclear compounds from a composite N-donor ligand.

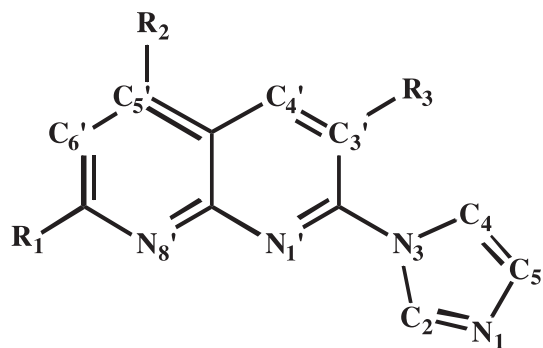
We have employed naphthyridine–imidazole hybrid ligands (Scheme 1) for the synthesis of multinuclear compounds. The naphthyridine and imidazole nitrogens offer prospect for multi-metal assemblies. The square-planar metal component 'Rh(COD)' (COD = 1,5-cyclooctadiene) has been chosen as the metal-containing unit. By judicious alteration in the ligand framework, and in the metal coordination sphere as well, dinuclear $[\text{Rh}(\text{COD})\text{Cl}]_2(\mu-L^1)$ (**1**), tetranuclear macrocycle $[\text{Rh}(\text{COD})L^1]_4[\text{ClO}_4]_4$ (**2**) and polymeric $\{\text{Rh}(\text{COD})(L^2)\}_n(\text{PF}_6)_n$ (**3**) have been synthesized (Scheme 2). In this report, we make an attempt to rationalize their structures based on the ligand conformation and the metal-ion geometry.

2. Results and discussion

2.1. $[\text{Rh}(\text{COD})\text{Cl}]_2(\mu-L^1)$ (**1**)

Addition of L^1 to the $[\text{Rh}(\text{COD})\text{Cl}]_2$ in dichloromethane disrupts the dimeric structure and affords **1** in high yield. Molecular structure of **1** consists of two 'Rh(COD)Cl' units bridged by L^1 (Fig. 1). The terminal nitrogens of imidazolyl (N_1) and naphthyridine (N_8') units bind to two independent Rh centers. The coordinating geometry around each Rh center is square planar and the metrical parameters are similar to those reported for Rh^I -COD compounds [32]. The angle between the naphthyridine (NP) plane and the

* Corresponding author. Tel.: +91 512 259 7336; fax: +91 512 259 7436.
E-mail address: jbera@iitk.ac.in (J.K. Bera).



Scheme 1. Ligands used in the present study and the numbering scheme.

imidazole (Im) plane is 3.9° (φ N2–C30–N3–C33 = $2.9(5)^\circ$). The non-bonded Rh...Rh distance is 6.1004(7) Å.

The ^1H NMR of **1** reveals a 2:1 composition of 'Rh(COD)' and L^1 . However, the NMR spectrum exhibits two sets of NP protons in the ratio 1:0.7, clearly indicating a mixture of compounds in solution (see Fig. S1). The methyl protons appear as two singlets at δ 2.67, 2.71 ppm. In addition, broad signals are observed for COD protons at δ 1.84, 2.49, 4.21, 4.59 ppm. Based on the NMR data, the presence of $\text{Rh}(\text{COD})\text{Cl}(\kappa\text{N}_1\text{-}L^1)$, $\text{Rh}(\text{COD})\text{Cl}(\kappa\text{N}_8\text{-}L^1)$ and the original dimer $[\text{Rh}(\text{COD})\text{Cl}]_2$ is proposed. Interestingly, the ESI-MS exhibits high-intensity signals at 905, 681, 659, 435 attributed to $\{\text{Rh}_2(\text{COD})_2(\text{Cl})(L^1)_2\}^+$, $\{\text{Rh}_2(\text{COD})_2(\text{Cl})(L^1)\}^+$, $\{\text{Rh}(\text{COD})(L^1)_2\}^+$, $\{\text{Rh}(\text{COD})(L^1)\}^+$, respectively. The assignment is based on mass and isotropic distribution pattern.

2.2. $[\text{Rh}(\text{COD})L^1]_4[\text{ClO}_4]_4$ (**2**)

Removal of chlorides from $[\text{Rh}(\text{COD})\text{Cl}]_2$ by TiClO_4 and subsequent addition of L^1 provided a cyclic tetramer $[\text{Rh}(\text{COD})L^1]_4[\text{ClO}_4]_4$ (**2**). Molecular structure of **2** is confirmed by X-ray crystallography. The tetracationic core consists of four 'Rh(COD)' units bridged by four L^1 ligands (Fig. 2(a)). The molecule crystallizes in the tetragonal I41/a space group and only one 'Rh(COD) L^1 ' is observed in the asymmetric unit. Each Rh is connected to the neighboring metal by L^1 ligand through the terminal nitrogens of the Im and NP units. The four metals form an equilateral quadrangle of 8.5652(7) Å, each Rh makes an angle of $87.742(1)^\circ$ with two adjoining metals, and four metals do not reside on the same plane (see Fig. 2(b)). The L^1 adapts a planar configuration (φ N2–C10–N3–

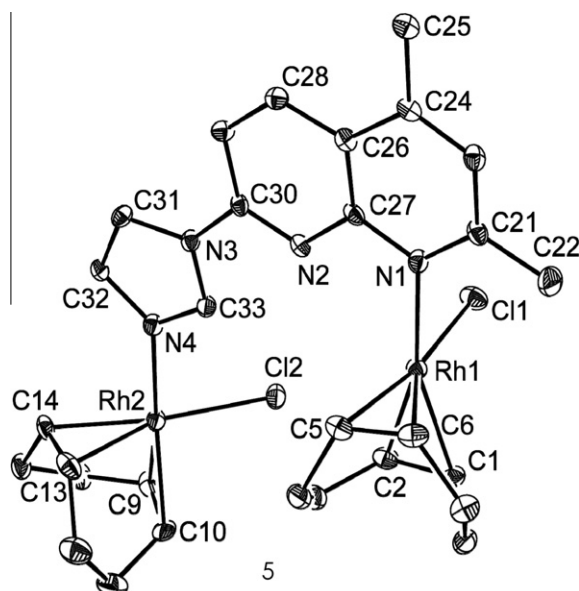


Fig. 1. ORTEP diagram (50% probability thermal ellipsoid) of **1** with important atoms labeled. Hydrogen atoms omitted for the sake of clarity. Selected bond distances (Å) and angles ($^\circ$): Rh1–N1 2.124(3), Rh1–Cl1 2.3833(11), Rh1–C1 2.104(4), Rh1–C2 2.106(4), Rh1–C5 2.123(4), Rh1–C6 2.128(4), Rh2–C12 2.3910(10), Rh2–N4 2.105(3), Rh2–C9 2.094(4), Rh2–C10 2.103(4), Rh2–C13 2.127(4), Rh2–C14 2.137(4), N1–Rh1–Cl1 86.95(9), N4–Rh2–Cl2 90.64(9), N2–C30–N3–C33 2.9(5), Rh1...Rh2 6.1004(7).

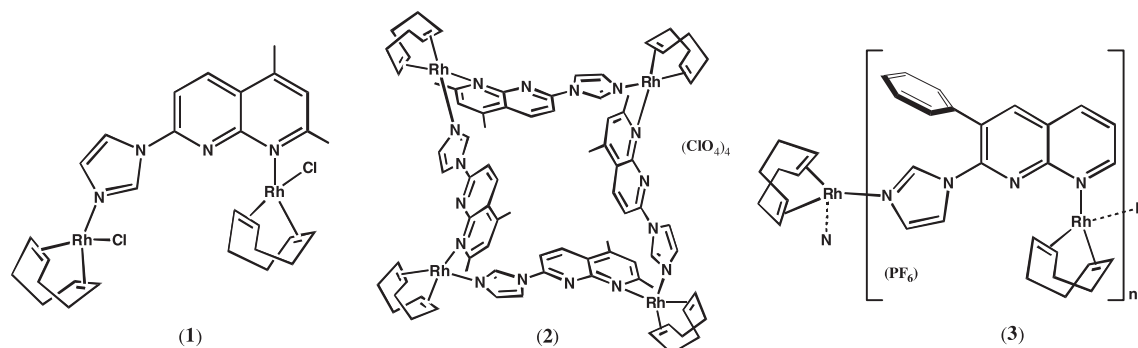
$\text{C12} = 0.1(6)^\circ$). The Rh...Rh distance is 8.5652(7) Å, longer than the corresponding metal...metal distance in **1** by 2.47 Å.

The tetrameric compound **2** is also obtained from the dimer **1**. Treatment of **1** by Ti^{I} salt and subsequent addition of one equivalent of L^1 provided the cyclic tetramer **2**. Evidently, the removal of chloride allows the propagation of the structure aided by the linker L^1 culminating in a cyclic tetranuclear structure.

The iridium analog $[\text{Ir}(\text{COD})L^1]_4[\text{OTf}]_4$ has been synthesized following a similar procedure using $[\text{Ir}(\text{COD})\text{Cl}]_2$, TiOTf and L^1 . The ORTEP diagram and the important bond parameters are provided in the supporting information.

Although the coordination motif of the L^1 is identical in both dimer structure **1** and tetrameric structure **2**, some significant differences are noted. The 'parallel' and 'perpendicular' disposition of the coordinating nitrogens are the characteristic features of compounds **1** and **2** (Fig. 3). This results in different metal...metal separations (6.1004(7) for **1** and 8.5652(7) Å for **2**).

All NP and COD protons exhibit broad signals in the ^1H NMR spectrum. The ESI-MS spectrum of complex **2** reveals signal at



Scheme 2. Line drawings of metallo-assemblies **1–3**.

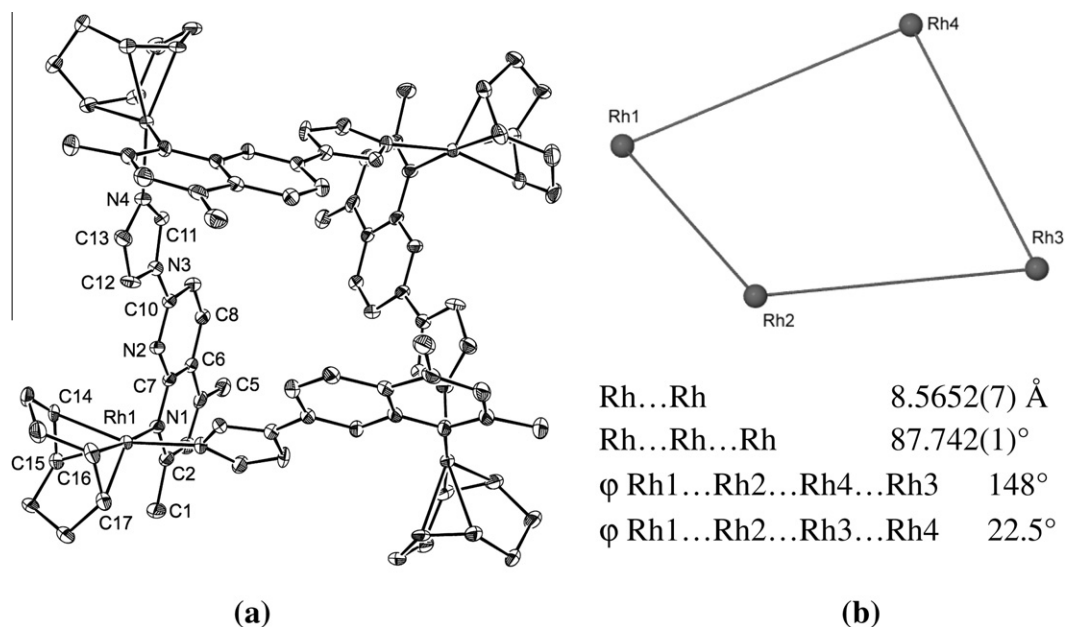


Fig. 2. (a) ORTEP diagram (30% probability thermal ellipsoid) of the tetracationic unit $[\text{Rh}(\text{COD})\text{L}^1]_4$ in compound **2** with important atoms labeled. Hydrogen atoms omitted for the sake of clarity. Selected bond distances (Å) and angles ($^\circ$): Rh1–N4 2.099(3), Rh1–C18 2.109(5), Rh1–C14 2.124(4), Rh1–C19 2.138(6), Rh1–C15 2.150(4), Rh1–N1 2.165(4), N4–Rh1 2.099(3), N4–Rh1–N1 87.41(14), C18–Rh1–N1 145.21(18), C14–Rh1–N1 96.3(2), C19–Rh1–N1 175.70(18), C15–Rh1–N1 89.92(18), N4–Rh1–C18 90.39(17), N4–Rh1–C14 158.73(18), N4–Rh1–C19 93.62(17), N4–Rh1–C15 163.25(17). (b) The skeletal arrangement of Rh_4 moiety.

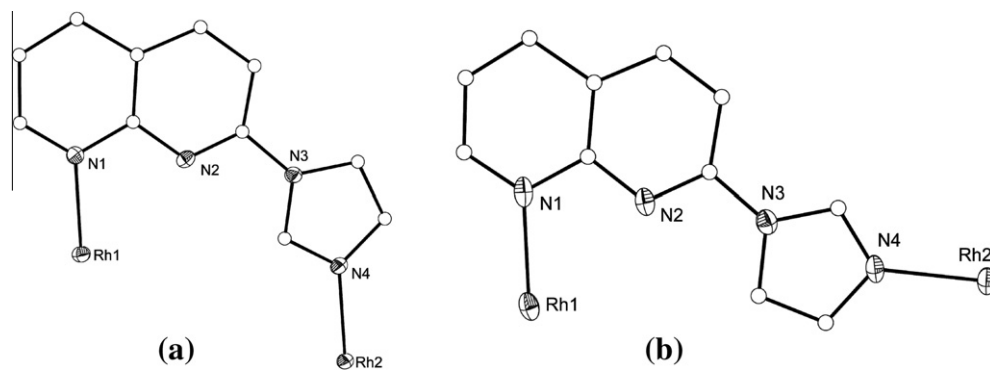


Fig. 3. The 'parallel' and 'perpendicular' dispositions of L^1 in compounds **1** (a) and **2** (b).

m/z 1221 ($z = 1$) corresponding to a species $[\text{Rh}_3(\text{COD})_3(\text{L}^1)_2 - (\text{CH}_3\text{CN})(\text{ClO}_4)]^+$.

2.3. $\{\text{Rh}(\text{COD})(\text{L}^2)\}_n(\text{PF}_6)_n$ (**3**)

X-ray structures of **1** and **2** reveal a planar arrangement of L^1 ligand. We introduced a phenyl ring at C_3 position with an intention to disrupt the planarity, and examine the structural perturbation. Reaction of $[\text{Rh}(\text{COD})\text{Cl}]_2$, TIPF_6 and **1**, following a procedure identical to that of **2**, resulted in an one-dimensional zig-zag chain structure $[\text{Rh}(\text{COD})\text{L}^2]_n[\text{PF}_6]_n$ (**3**). Molecular structure of **3**, determined by X-ray crystallography, reveals a polymeric chain consisting of alternate ' $\text{Rh}(\text{COD})$ ' and L^2 (Fig. 4). The non-bonded Rh...Rh distance is 8.0110(11) Å. The coordination motif of L^2 is the same as for L^1 , which is binding through the terminal NP and Im nitrogens. The disposition of the coordinating nitrogens is 'perpendicular'. The angle between NP plane and Im plane is 42.2° (ϕ N2–C18–N3–C26 = 34.9°), and the phenyl ring rotates away from the NP plane (Inter-planar angle = 51.5° ; ϕ C18–C17–C19–C24 = 51.9°) (Fig. 5). The deviation of NP and Im rings from planarity leads to the open-chain structure.

The ^1H NMR spectrum exhibits well resolved signals indicating a 1:1 composition of ' $\text{Rh}(\text{COD})$ ' and L^2 in CD_3CN . ESI-MS spectrum of complex **3** exhibits signal at m/z 483 and 755 ($z = 1$) attributed to $[\text{Rh}(\text{COD})\text{L}^2]^+$ and $[\text{Rh}(\text{COD})(\text{L}^2)_2]^+$, respectively. Interestingly, the signal for the latter complex is the most intense signal (100%) in the mass spectrum.

2.4. $\{\text{Mo}_2(\text{OAc})_4(\text{L}^2)\}_n$ (**4**)

The coordination chemistry of L^2 was further studied with a dimolybdenum(II) compound $[\text{Mo}_2(\text{OAc})_4]$. The strong trans influence of the Mo–Mo quadruple bond allows weak N coordination at axial sites with minimum perturbation on the ligand [33,34]. The polymeric structure of compound **4** of empirical formula $\{\text{Mo}_2(\text{OAc})_4\text{L}^2\}_n$ consists of alternate ' $\text{Mo}_2(\text{OAc})_4$ ' and L^2 units. Two neighboring ' $\text{Mo}_2(\text{OAc})_4$ ' molecules are linked by L^2 through the NP nitrogen and Im nitrogen as depicted in Fig. 6. The 'parallel' disposition of the coordinating nitrogens is observed in this structure. The Mo–N distances (2.628(1) and 2.656(1) Å) are characteristically long. The NP and Im rings deviate from planarity and the inter-planar angle is 24.46° . The extent of deviation is smaller than

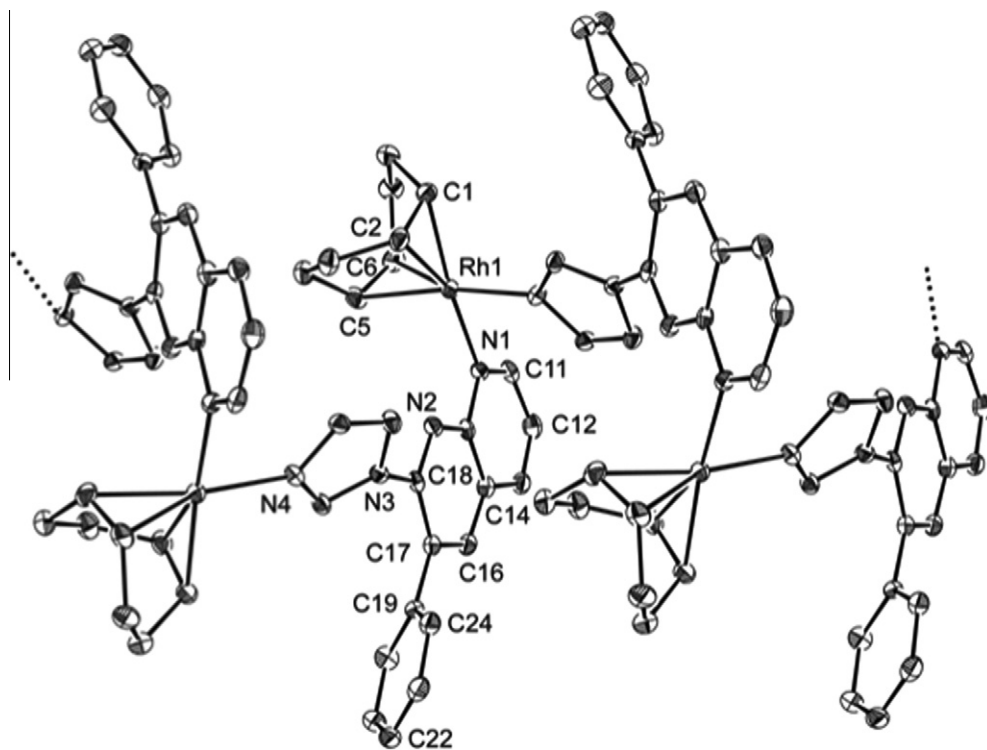


Fig. 4. ORTEP diagram (40% probability thermal ellipsoid) of the cationic unit $[\text{Rh}(\text{COD})\text{L}^2]^+$ in compound **3** with important atoms labeled. Hydrogen atoms omitted for the sake of clarity. Selected bond distances (Å) and angles ($^\circ$): Rh1–C6 2.108(4), Rh1–N4 2.116(3), Rh1–C2 2.119(4), Rh1–N1 2.128(3), Rh1–C1 2.136(4), Rh1–C5 2.138(4), C6–Rh1–N4 92.11(13), C6–Rh1–C2 99.43(16), N4–Rh1–C2 155.26(13), C6–Rh1–N1 153.82(14), N4–Rh1–N1 88.74(11), C2–Rh1–N1 90.32(14), C6–Rh1–C1 82.84(15), N4–Rh1–C1 166.75(13), C2–Rh1–C1 37.95(14), N1–Rh1–C1 90.45(13), C6–Rh1–C5 38.47(15), N4–Rh1–C5 93.67(12), C2–Rh1–C5 82.35(15), N1–Rh1–C5 167.47(13), C1–Rh1–C5 89.97(15) Rh1...Rh1 8.0110(11). Symmetry code: $1/2 + X, 3/2 - Y, 2 - Z$.

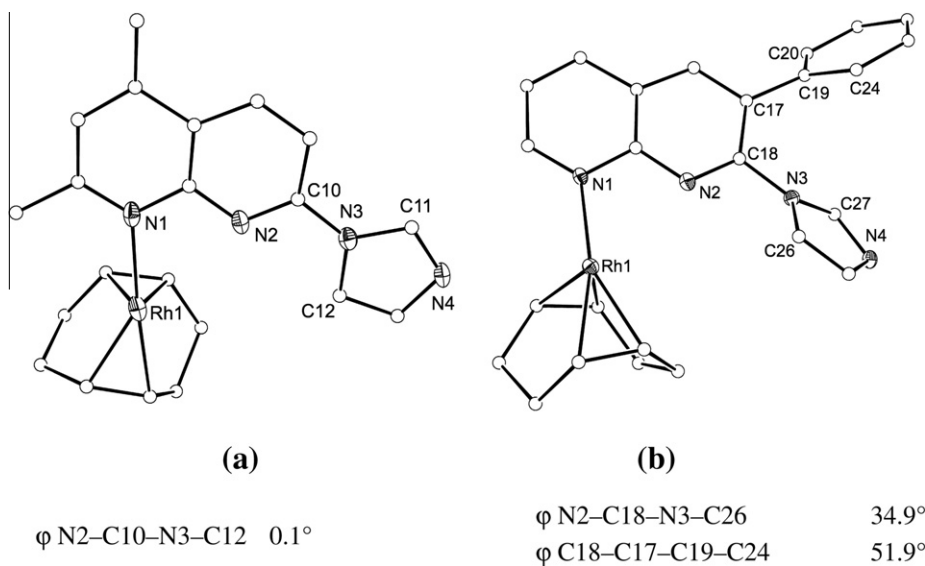


Fig. 5. The configurations of L^1 and L^2 ligands in compounds **2** (a) and **3** (b), respectively.

that observed in **3**. The Ph ring is also rotated away from the NP plane as reflected in the C18–C17–C22–C27 dihedral angle $45.4(5)^\circ$.

3. Summary and conclusions

Table 1 summarizes the relevant details of compounds **1–4**. Addition of L^1 to $[\text{Rh}(\text{COD})\text{Cl}]_2$ disrupts the chloro-bridged structure

and forms dinuclear complex $[\text{Rh}(\text{COD})\text{Cl}]_2(\mu\text{-L}^1)$ (**1**). Removal of chloride from the metal coordination sphere allows further propagation of the structure resulting in a metallamacrocycle $\{[\text{Rh}(\text{COD})\text{L}^1]_4\}^{4+}$. Use of L^2 under identical condition, however, afforded an infinite cationic zig-zag chain $\{[\text{Rh}(\text{COD})(\text{L}^2)]_n\}^{n+}$. A neutral polymeric chain compound of empirical formula $\{\text{Mo}_2(\text{OAc})_4(\text{L}^2)\}$ is obtained by treating L^2 with $[\text{Mo}_2(\text{OAc})_4]$. In all these cases, the imidazole nitrogen and one of the naphthyridine nitrogen

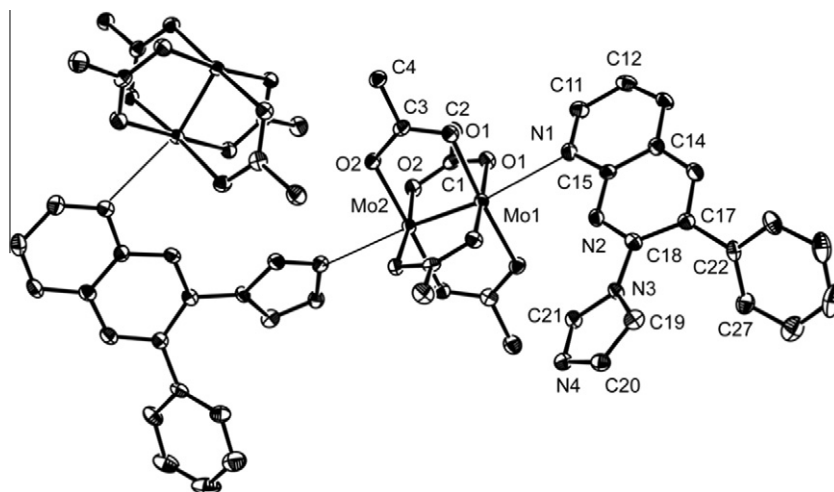


Fig. 6. ORTEP diagram (50% probability thermal ellipsoid) of a fragment in the chain compound $[\text{Mo}_2(\text{OAc})_4(\text{L}^2)]_n$ (**4**) with important atoms labeled. Hydrogen atoms omitted for the sake of clarity. Selected bond distances (Å) and angles ($^\circ$): Mo1–N1 2.628(3), Mo1–Mo2 2.1098(4), Mo1–O1 2.112(3), Mo1–O7 2.117(3), Mo1–O5 2.125(3), Mo1–O3 2.158(3), Mo2–O4 2.101(3), Mo2–O6 2.123(2), Mo2–O2 2.123(3), Mo2–O8 2.132(3), Mo2–Mo1–N1 160.18(7), O1–Mo1–N1 85.93(10), O7–Mo1–N1 90.06(10), O5–Mo1–N1 108.02(10), O3–Mo1–N1 71.31(10).

Table 1
Relevant structural details in compounds **1–4**.

Compound	Ligand	Structure	Ligand configuration	Rh...Rh (Å)	ϕ^a ($^\circ$)
$[\text{Rh}(\text{COD})\text{Cl}]_2(\mu\text{-L}^1)$ (1)	L^1	Dimer	Parallel	6.1004(7)	3.9
$[\text{Rh}(\text{COD})\text{L}^1]_4[\text{ClO}_4]_4$ (2)	L^1	Equilateral quadrangle	Perpendicular	8.5652(7)	1.69
$[\text{Rh}(\text{COD})(\text{L}^2)]_n(\text{PF}_6)_n$ (3)	L^2	Zig-zag polymer chain	Perpendicular	8.0110(11)	42.22
$[\text{Mo}_2(\text{OAc})_4(\text{L}^2)]_n$ (4)	L^2	Zig-zag polymer chain	Parallel	–	24.46

^a NP–Im inter-planar angle.

(away from the imidazole substituent) bind the metal. These nitrogens adopt ‘parallel’ conformation in compounds **1**, **4** and ‘perpendicular’ conformation in compounds **2**, **3** (Table 1). The free rotation of NP and Im rings around the C–N single bond allows these two unique orientations causing different Rh...Rh separations; the ‘parallel’ and ‘perpendicular’ arrangements result in shorter and longer metal...metal separations. The L^1 adopts a planar structure, whereas L^2 is non-planar. The non-planarity of L^2 is attributed to the open-chain structure of **3**, whereas a cyclic structure **2** is obtained for planar L^1 . In compound **4**, the L^2 ligand exhibits ‘parallel’ disposition of the coordinating nitrogens, and the NP and Im rings are non-planar though the extent of deviation is comparatively less. In conclusion, the present study illustrates that judicious alteration in the ligand framework and/or adjustment in the metal coordination sphere are possible ways to access self-assembled structures of varied nuclearity and diverse topology.

3.1. General procedures and materials

All reactions were carried out under an inert dinitrogen atmosphere with the use of standard Schlenk-line techniques. Solvents were dried by conventional methods, distilled over nitrogen, and deoxygenated prior to use. $[\text{Ir}(\text{COD})\text{Cl}]_2$ [35,36], $[\text{Rh}(\text{COD})\text{Cl}]_2$ [37], $\text{Mo}_2(\text{CH}_3\text{COO})_4$ [38–40], 2-imidazolyl-5,7-dimethyl-1,8-naphthyridine (L^1) and 2-imidazolyl-3-phenyl-1,8-naphthyridine (L^2) [41] were prepared by following literature procedures.

3.2. Physical measurements

Elemental analyses were carried out using a Thermoquest CE instruments model EA/110 CHNS-O elemental analyzer. ESI-MS spectra were recorded on a Waters Micromass Quattro Micro

triple-quadrupole mass spectrometer. The ^1H NMR spectrum was obtained on a JEOL JNM-LA 500 MHz spectrophotometer. Infrared spectra were recorded on a Bruker Vertex 70 FTIR spectrophotometer in the ranges from 400 to 4000 cm^{-1} using KBr pellets.

3.3. X-ray data collection and refinement

Single-crystal X-ray studies were performed on a CCD Bruker SMART APEX diffractometer equipped with an Oxford Instruments low-temperature attachment. All data were collected at 100(2) K using graphite monochromated $\text{Mo K}\alpha$ radiation (λ_{air} 0.71073 Å). The frames were indexed, integrated, and scaled using the SMART and SAINT software packages [42], and the data were corrected for absorption using the SADABS programs [43]. Structures were solved and refined with the SHELX suite of programs [44,45] as implemented in X-seed [46,47]. The ‘‘SQUEEZE’’ option in PLATON program [48] was used to remove a disordered solvent molecule from the overall intensity data of compounds **2** and **5**. The figures were drawn using ORTEP [49]. All the hydrogen atoms were included at geometrically calculated positions in the final stages of the refinement and were refined according to the ‘‘riding model’’. All non-hydrogen atoms were refined with anisotropic thermal parameters unless mentioned otherwise. Pertinent crystallographic data for compounds **1–4** are summarized in Table 2.

3.4. Synthesis of $[\text{Rh}(\text{COD})\text{Cl}]_2(\mu\text{-L}^1)$ (**1**)

L^1 (30 mg, 0.134 mmol) was added to a dichloromethane solution (10 mL) of $[\text{RhCl}(\text{COD})]_2$ (65 mg, 0.132 mmol) and the yellow mixture was stirred for 12 h at room temperature. The resulting orange solution was concentrated under vacuum and 15 mL of diethyl ether were added with stirring to induce precipitation.

Table 2
Crystallographic data and pertinent refinement parameters for compounds 1–4.

	1. CH ₂ Cl ₂	2	3	4
Empirical formula	C ₃₀ H ₃₈ Cl ₄ N ₄ Rh ₂	C ₈₄ H ₉₆ Cl ₄ N ₁₆ O ₁₆ Rh ₄	C ₂₅ H ₂₄ F ₆ N ₄ PRh	C ₂₅ H ₂₄ Mo ₂ N ₄ O ₈
Formula weight	802.26	2139.21	628.36	700.36
Crystal system	triclinic	tetragonal	orthorhombic	orthorhombic
Space group	<i>P</i> $\bar{1}$	<i>I</i> 41/a	<i>P</i> 2(1)2(1)2(1)	<i>Pna</i> 21
<i>a</i> (Å)	10.2847(10)	16.0732(11)	9.694(2)	8.6412(7)
<i>b</i> (Å)	11.0185(11)	16.0732(11)	12.358(3)	24.883(2)
<i>c</i> (Å)	16.3603(16)	37.675(5)	19.765(4)	12.0562(10)
α (°)	92.891(2)			
β (°)	108.210(2)	90.00	90.00	90.00
γ (°)	114.8180(10)			
<i>V</i> (°)	1562.6(3)	9733.2(15)	2367.9(9)	2592.3(4)
<i>Z</i>	2	4	4	4
ρ_{calc} (g cm ⁻³)	1.705	1.460	1.763	1.795
μ (mm ⁻¹)	1.426	0.844	0.860	1.025
<i>F</i> (0 0 0)	808	4352	1264	1400
Reflections collected	13826	43698	20950	22101
Independent	7371	5964	5775	6378
Observed [<i>I</i> > 2 σ (<i>I</i>)]	5747	4174	5127	5653
Number of variables	363	284	334	356
Goodness-of-fit (GOF)	1.075	1.110	1.119	1.082
<i>R</i> _{int}	0.0262	0.0709	0.0611	0.0471
Final <i>R</i> indices [<i>I</i> > 2 σ (<i>I</i>)] ^a	<i>R</i> ₁ = 0.0369	0.0607	0.0338	0.0314
	<i>wR</i> ₂ = 0.0811	0.1668	0.0482	0.0675
<i>R</i> indices (all data) ^a	<i>R</i> ₁ = 0.0553	0.0886	0.0662	0.0460
	<i>wR</i> ₂ = 0.1032	0.1873	0.0784	0.0758

$$^a R_1 = \sum ||F_o| - |F_c|| / \sum |F_o| \text{ with } F_o^2 > 2\sigma(F_o^2). \quad wR_2 = [\sum w(|F_o|^2 - |F_c|^2)|^2 / \sum |F_o|^2]^{1/2}.$$

Then it was dried in vacuum. Crystals were grown by layering hexane over dichloromethane solution of the complex. Yield: 86 mg (91%). *Anal. Calc.* for C₂₉H₃₆Cl₂N₄Rh₂: C, 48.56; H, 5.06; N, 7.81. Found: C, 48.49; H, 4.92; N, 7.80%. IR (KBr pellet): ν (COD) 2925 cm⁻¹. ¹H NMR (CD₂Cl₂, δ , ppm): 9.27, 9.01 (s, 2H, Im), 8.52, 7.97 (s, 2H, Im), 8.51, 8.46 (d, 2H, NP), 7.69, 7.60 (d, 2H, NP), 7.32, 7.21 (s, 2H, NP), 7.24, 7.05 (s, 2H, Im), 4.59, 4.21 (br, 4H, COD), 2.71, 2.67 (s, 12H, Me), 2.49 (br, 10H, COD), 1.84 (br, 10H, COD). ESI-MS: *m/z* 681 [Rh₂(COD)₂(Cl)(L¹)]⁺.

3.5. Synthesis of [Rh(COD)L¹]₄(ClO₄)₄ (2)

TiClO₄ (86 mg, 0.284 mmol) was added to an acetonitrile solution (10 mL) of [RhCl(COD)]₂ (70 mg, 0.142 mmol) and the yellow mixture was stirred for 30 min. The TiCl was removed by Schlenk filtration, then L¹ (64 mg, 0.284 mmol) was added to the filtrate and the mixture was stirred for 16 h at room temperature. The resulting orange solution was concentrated under vacuum and 15 mL of diethyl ether were added with stirring to induce precipitation. Then it was dried in vacuum. Crystals were grown by layering hexane over dichloromethane solution of the complex. Yield: 134 mg (88%). *Anal. Calc.* for C₈₄H₉₆Cl₄N₁₆O₁₆Rh₄: C, 47.16; H, 4.52; N, 10.48. Found: C, 47.05; H, 4.32; N, 10.31%. IR (KBr pellet): ν (COD) 2928 cm⁻¹; ν (ClO₄⁻) 1084 cm⁻¹. ¹H NMR (CD₃CN, δ , ppm): 9.73 (br, 1H, Im), 8.66 (br, 1H, NP), 7.74 (br, 1H, NP), 7.53 (br, 1H, NP), 7.24 (br, 1H, Im), 7.03 (br, 1H, Im), 4.61 (br, 4H, COD), 4.20 (br, 4H, COD), 2.71 (s, 3H, Me), 2.65 (s, 3H, Me), 2.32 (br, 4H, COD). ESI-MS: *m/z* 1221 [Rh₃(COD)₃(L¹)₂(CH₃CN)(ClO₄)]⁺.

3.6. Synthesis of {Rh(COD)(L²)_n(PF₆)_n} (3)

TIPF₆ (99 mg, 0.283 mmol) was added to an acetonitrile solution (10 mL) of [RhCl(COD)]₂ (70 mg, 0.142 mmol) and the yellow mixture was stirred for 30 min. The TiCl was removed by Schlenk filtration, then L² (77 mg, 0.282 mmol) was added to the filtrate and the mixture was stirred for 12 h at room temperature. The resulting orange solution was concentrated under vacuum and 15 mL of diethyl ether were added with stirring to induce precipi-

tion. Then it was dried in vacuum. Crystals were grown by layering hexane over dichloromethane solution of the complex. Yield: 157 mg (88%). *Anal. Calc.* for C₂₅H₂₄F₆N₄PRh: C, 47.79; H, 3.85; N, 8.92. Found: C, 47.49; H, 3.74; N, 8.79%. IR (KBr pellet): ν (COD) 2923 cm⁻¹, ν (PF₆⁻) 843 cm⁻¹. ¹H NMR (CD₃CN, δ , ppm): 9.15 (s, 1H, NP), 8.52 (s, 1H, NP), 8.45 (d, 1H, NP), 7.68 (br, 1H, Im), 7.68 (br, 1H, NP), 7.41 (s, 3H, Ph), 7.35 (s, 1H, Im), 7.28 (d, 2H, Ph), 6.90 (s, 1H, Im), 4.25 (br, 4H, COD), 2.42 (br, 4H, COD), 1.25 (br, 4H, COD). ESI-MS: *m/z* 755 [Rh(COD)(L²)₂]⁺.

3.7. Synthesis of [Mo₂(OAc)₄(L²)_n] (4)

L² (76 mg, 0.28 mmol) was added to an acetonitrile solution (10 mL) of Mo₂(OAc)₄ (60 mg, 0.14 mmol) and the yellow mixture was stirred for 12 h at room temperature. The color was changed from yellow to reddish brown. The resulting solution was concentrated under vacuum and 15 mL of diethyl ether were added with stirring to induce precipitation. Then it was dried in vacuum. Crystals were grown by layering hexane over dichloromethane solution of the complex. Yield: 113 mg (83%). *Anal. Calc.* for C₂₅H₂₄N₄O₈Mo₂: C, 42.87; H, 3.45; N, 8.00. Found: C, 42.32; H, 3.21; N, 7.91%. IR (KBr pellet): ν (CH₃COO⁻) 1432 cm⁻¹. ¹H NMR (CD₃CN, δ , ppm): 9.13 (dd, 1H, NP), 8.67 (s, H, NP), 8.56 (dd, H, NP), 7.73 (s, H, Im), 7.70 (s, H, NP), 7.43 (br, 3H, Ph), 7.32 (br, 2H, Ph), 7.22 (s, H, Im), 6.93 (s, H, Im), 2.47 (s, 12H, CH₃COO⁻).

Acknowledgements

J.K.B. thanks DST India for support of this research. D.D. thanks CSIR, India and S.M.W.R. thanks UGC, India for fellowships.

Appendix A. Supplementary material

CCDC 808933, 808934, 808935 and 808936 contain the supplementary crystallographic data for compounds 1, 2, 3 and 4, respectively. These data can be obtained free of charge from The Cambridge Crystallographic Data Centre via www.ccdc.cam.ac.uk/data_request/cif. Supplementary data associated with this article

can be found, in the online version, at [doi:10.1016/j.ica.2011.03.033](https://doi.org/10.1016/j.ica.2011.03.033).

References

- [1] S. Ma, D. Sun, M. Ambrogio, J.A. Fillinger, S. Parkin, H.-C. Zhou, *J. Am. Chem. Soc.* 129 (2007) 1858.
- [2] S. Ma, D. Sun, J.M. Simmons, C.D. Collier, D. Yuan, H.-C. Zhou, *J. Am. Chem. Soc.* 130 (2008) 1012.
- [3] S. Barman, H. Furukawa, O. Blacque, K. Venkatesan, O.M. Yaghi, H. Berke, *Chem. Commun.* 46 (2010) 7981.
- [4] H. Furukawa, O.M. Yaghi, *J. Am. Chem. Soc.* 131 (2009) 8875.
- [5] M. Yoshizawa, J.K. Klosterman, M. Fujita, *Angew. Chem.* 48 (2009) 3418.
- [6] M.D. Pluth, R.G. Begman, K.N. Raymond, *Acc. Chem. Res.* 42 (2009) 1650.
- [7] M. Yoshizawa, M. Tamura, M. Fujita, *Science* 312 (2006) 251.
- [8] M.D. Pluth, R.G. Bergman, K.N. Raymond, *Science* 316 (2007) 85.
- [9] R. Bagai, G. Christou, *Chem. Soc. Rev.* 38 (2009) 1011.
- [10] M. Morimoto, H. Miyasaka, M. Yamashita, M. Irie, *J. Am. Chem. Soc.* 131 (2009) 9823.
- [11] E.E. Moushi, C. Lampropoulos, W. Wernsdorfer, V. Nastopoulos, G. Christou, A.J. Tasiopoulos, *J. Am. Chem. Soc.* 132 (2010) 16146.
- [12] Y.-R. Zheng, Z. Zhao, M. Wang, K. Ghosh, J.B. Pollock, T.R. Cook, P.J. Stang, *J. Am. Chem. Soc.* 132 (2010) 16873.
- [13] F. D'Souza, N.K. Subbaiyan, Y. Xie, J.P. Hill, K. Ariga, K. Ohkubo, S. Fukuzumi, *J. Am. Chem. Soc.* 131 (2009) 16138.
- [14] J.L. Sessler, E. Karnas, S.K. Kim, Z. Ou, M. Zhang, K.M. Kadish, K. Ohkubo, S. Fukuzumi, *J. Am. Chem. Soc.* 130 (2008) 15256.
- [15] S.J. Lee, W. Lin, *Acc. Chem. Res.* 41 (2008) 521.
- [16] J.W. Steed, *Chem. Soc. Rev.* 38 (2009) 506.
- [17] K.-I. Yamashita, M. Kawano, M. Fujita, *Chem. Commun.* (2007) 4102.
- [18] Y. Liu, X. Wu, C. He, Y. Jiao, C. Duan, *Chem. Commun.* (2009) 7554.
- [19] D.J. Tranchemontagne, J.L. Mendoza-Cortés, M. O'Keefe, O.M. Yaghi, *Chem. Soc. Rev.* 38 (2009) 1257.
- [20] N.L. Rosi, J. Kim, M. Eddaoudi, B. Chen, M. O'Keefe, O.M. Yaghi, *J. Am. Chem. Soc.* 127 (2005) 1504.
- [21] O.M. Yaghi, M. O'Keefe, N.W. Ockwig, H.K. Chae, M. Eddaoudi, J. Kim, *Nature* 423 (2003) 705.
- [22] S.R. Seidel, P.J. Stang, *Acc. Chem. Res.* 35 (2002) 972.
- [23] T. Chen, G.-B. Pan, H. Wettach, M. Fritzsche, S. Hger, L.-J. Wan, H.-B. Yang, B.H. Northrop, P.J. Stang, *J. Am. Chem. Soc.* 132 (2010) 1328.
- [24] J.K. Bera, J. Bacsa, K.R. Dunbar, in: R.B. King (Ed.), *Encyclopedia of Inorganic Chemistry*, second ed., John Wiley & Sons, New York, 2005.
- [25] Y. Sunatsuki, Y. Motoda, N. Matsumoto, *Coord. Chem. Rev.* 226 (2002) 199.
- [26] E. Colacio, M. Ghazi, R. Kivekäs, M. Klinga, F. Lloret, J.M. Moreno, *Inorg. Chem.* 39 (2000) 2770.
- [27] S. Ghosh, P.S. Mukherjee, *Inorg. Chem.* 48 (2009) 2605.
- [28] R. Kieltyka, P. Englebienne, J. Fakhoury, C. Autexier, N. Moitessier, H.F. Sleiman, *J. Am. Chem. Soc.* 130 (2008) 10040.
- [29] J.K. Bera, B.W. Smucker, R.A. Walton, K.R. Dunbar, *Chem. Commun.* (2001) 2562.
- [30] J.K. Bera, J. Bacsa, B.W. Smucker, K.R. Dunbar, *Eur. J. Inorg. Chem.* (2004) 368.
- [31] K. Severin, *Chem. Commun.* (2006) 3859.
- [32] M. Martín, O. Torres, E. Oñate, E. Sola, L.A. Oro, *J. Am. Chem. Soc.* 127 (2005) 18074. and references therein.
- [33] F.A. Cotton, C.A. Murillo, R.A. Walton, *Multiple Bonds between Metal Atoms*, third ed., Springer Science and Business Media, New York, 2005.
- [34] F.A. Cotton, C.A. Murillo, R.A. Walton, *Multiple Bonds between Metal Atoms*, second ed., Clarendon Press, Oxford, UK, 1993.
- [35] J.L. Herde, J.C. Lambert, C.V. Senoff, *Inorg. Synth.* 15 (1974) 18.
- [36] F.A. Cotton, P. Lahuerta, M. Sanau, W. Schwotzer, *Inorg. Chim. Acta* 120 (1986) 153.
- [37] G. Giordano, R.H. Crabtree, *Inorg. Synth.* 28 (1990) 90.
- [38] F.A. Cotton, Z.C. Mester, T.R. Webb, *Acta Cryst. B* 30 (1974) 2768.
- [39] A.B. Brignole, F.A. Cotton, *Inorg. Synth.* 13 (1972) 87.
- [40] D. Lawton, R.J. Mason, *J. Am. Chem. Soc.* 87 (1965) 921.
- [41] A. Sinha, S.M.W. Rahaman, M. Sarkar, B. Saha, P. Daw, J.K. Bera, *Inorg. Chem.* 48 (2009) 11114.
- [42] SAINT+ Software for CCD Diffractometers, Bruker AXS, Madison, WI, 2000.
- [43] G.M. Sheldrick, SADABS Program for Correction of Area Detector Data, University of Göttingen, Göttingen, Germany, 1999.
- [44] SHELXL Package v. 6.10; Bruker AXS, Madison, WI, 2000.
- [45] G.M. Sheldrick, SHELXS-86 and SHELXL-97, University of Göttingen, Göttingen, Germany, 1997.
- [46] J.L. Atwood, L.J. Barbour, *Cryst. Growth Des.* 3 (2003) 3.
- [47] L.J. Barbour, *J. Supramol. Chem.* 1 (2001) 189.
- [48] L. Spek, PLATON, University of Utrecht, The Netherlands, 2001.
- [49] L.J. Farrugia, *J. Appl. Cryst.* 30 (1997) 565.